Biochimica et Biophysica Acta, 1152 (1993) 155–160

BBAMEM 76105

Effect of ultrasound on the pH profiles in the unstirred layers near planar bilayer lipid membranes measured by microelectrodes

Peter Pohl [a,*], Yuri N. Antonenko [b] and Eike Rosenfeld [a]

[a] *Department of Medical Physics and Biophysics, Martin Luther University, Str. OdF 6, 06097 Halle (Germany) and* [b] *A.N. Belozersky Institute of Physico-Chemical Biology, Moscow State University, 119899 Moscow (Russia)*

(Received 5 April 1993)

Key words: Bilayer lipid membrane; Ultrasound; Unstirred layer; Weak acid; pH profile; Microelectrode

A pH shift in the unstirred layers (USLs) near a planar lipid bilayer membrane was induced by the diffusion of acetic acid along a concentration gradient. By means of a microelectrode technique it was shown that ultrasound decreases the thickness of the USL and that this reduction was much more pronounced on the side facing the ultrasound transducer than on the opposite side of the membrane. The effect depending on sound frequency and pressure is caused by the unidirectional fluid flow built up between transducer surface and membrane, the so-called quartz wind. Theoretical considerations based on the equations of the acoustic streaming near interfaces combined with the diffusion equation allow to predict the thickness of the USL if the sound field parameters are known.

Introduction

Unstirred layer (USL) effects play an essential role in transport across biological membranes. The layers adjacent to membranes act as additional diffusion barriers so that rapidly permeating substances could actually be rate-limited by diffusion within the USLs [1].

The reduction of the USL due to an unidirectional fluid flow developed in an ultrasonic field may be regarded as a possible mechanism for several bioeffects of ultrasound in vitro and in vivo. Such effects were found in different systems:

(a) catalytic reactions due to an enhanced mass transfer to the active center of immobilized enzymes [2–4],
(b) isolated cells showing an increasing permeability for various substances [5,6] and
(c) the permeation of pharmacological substances through membrane barriers [7].

Recently, in vitro studies have been undertaken to investigate the influence of ultrasound on the thickness of the USL near a bilayer lipid membrane (BLM). Using indirect methods like current measurements during the incorporation of gramicidin [8] and transmembrane potential measurements in the presence of a protonophore and an acetate gradient [9] it was found that ultrasound reduces the size of the USL δ in dependence on the sound intensity. These studies, however, were of qualitative character. In order to obtain quantitative results of the final thickness of the USL with an acceptable accuracy we now applied a microelectrode technique as proposed by Kasche and Kuhlmann [10]. First Antonenko and Bulychev measured pH profiles near BLM [11].

δ is defined in terms of the concentration gradient at the wall (see, e.g., Ref. 12):

$$\frac{|c_s - c_b|}{\delta} = \left.\frac{\partial c}{\partial x}\right|_{x=0} \quad (1)$$

where x is the distance from the membrane. c_s and c_b are the concentrations of the diffusing substances at the membrane surface and in the bulk solution, respectively. A possible solution of Eqn. 1 is the following exponential function:

$$c(x) = |c_s - c_b| e^{-x/\delta} + c_b \quad (2)$$

Knowing the sound field parameters the streaming velocity v can be estimated in the bulk volume [13]. Using Fick's law of diffusion it is possible to connect δ with the velocity v_v of the buffer movement towards the membrane within the viscous boundary layer. v_v is

* Corresponding author. Fax +49 345 671632.

assumed not to depend on the space coordinates parallel to the membrane and so do the steady state concentration of the diffusing substance [14]. Finally, the equation

$$v_v(x)\frac{dc}{dx} = D\frac{d^2c}{dx^2} \tag{3}$$

can be used to describe the balance between convection and diffusion [14], where D is the diffusion coefficient.

Materials and Methods

The BLMs were produced by a conventional method [15] in a hole, 1.2 mm in diameter, of a diaphragm of a PTFE chamber. The membrane forming solutions contained 20 mg phosphatidylcholine from soybeans (Sigma) and 10 mg cholesterol (Serva) in 1 ml of *n*-decane (Merck). A solution consisting of 1 mM Tris (Fluka), 1 mM Mes (Boehringer), 1 mM β-alanine (Merck) and 100 mM cholinchloride (Fluka) surrounded the bilayers. It was agitated by magnetic bars which stirred with the same velocity in all experiments.

Sodium acetate was added at one side of the membrane. The weak acid mediated proton flux through the membrane caused a concentration gradient of protons within the USL [16]. This gradient was measured as the potential difference between a pH microelectrode and a reference electrode, both of them placed in the buffer solution at the same side of the membrane. The reference electrode was positioned outside the soundfield. The voltage date were recorded by a Keithley 617 electrometer and transferred to a personal computer. The experimental arrangement is shown in Fig. 1.

The pH sensors were made of glass capillaries containing antimony. After pulling their tips had a diameter of about 5–10 μm. The pH electrodes were moved by a hydraulic microdrive manipulator. The touching of the membrane was indicated by a steep change of pH electrode potential [17]. Since the velocity of the electrode motion was known (4 μm s^{-1}) the position of the pH sensor relatively to the membrane could be determined at any instant of the experiment. The accuracy of the distance measurements was limited by the lack of a definite reference position for the membrane surface. It was assumed to be situated between the onset of the steep potential change and the breakdown of the BLM. The former was used as reference quantity. Usually, the withdrawal of the electrode started before the membrane was ruptured. A maximum total error of 8 μm was estimated.

In control experiments the membrane conductance was monitored via the electric current at a constant voltage of 50 mV. Therefore, reference electrodes were placed on both sides of the membrane and the built-in voltage source of the electrometer was used.

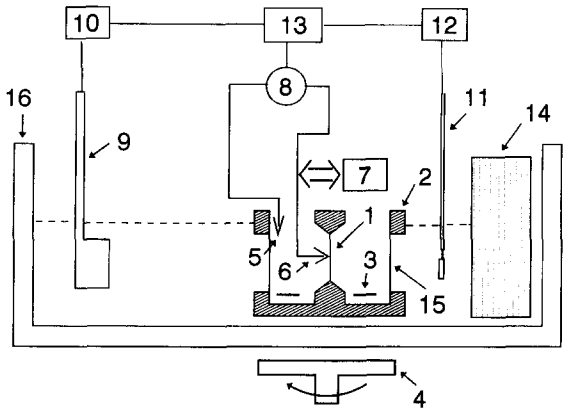

Fig. 1. Schematic of the experimental arrangement. 1, bilayer lipid membrane; 2, PTFE chamber; 3, magnetic stirrer bar; 4, stirrer; 5, reference electrode; 6, antimony electrode sensitive to H^+; 7, hydraulic microdrive; 8, electrometer (Keithley 617); 9, ultrasound transducer; 10, rf generator (LeCroy 9109) and broadband amplifier (rf power labs 161C); 11, ceramic hydrophone; 12, selective level meter (Anritsu ML422B/C); 13, personal computer; 14, absorber; 15, acoustic window; 16, water bath.

The ultrasonic fields were produced by broadband transducers obtained from Panametrics with resonance frequencies at 2.5, 5 and 10 MHz. The focal distance of the transducers was 50 mm. They were calibrated by means of a membrane polyvinylidene fluoride hydrophone purchased from NTR-Systems [18]. Additionally, one unfocussed broadband transducer with a resonance frequency of 3 MHz was used.

The ultrasound waves were transmitted through a small watertank to the PTFE chamber terminated by two acoustical windows made either of Parafilm or of polyethylene film. The BLM was positioned in the focus of the transducer under the control of a hydrophone. To exclude cavitational events during sound exposure the hydrophone was used to detect subharmonic acoustic signals. However, no emission was found. Recently, a rapid increase in streaming velocity was related to the harmonic content in the sound wave [19,20]. For that reason the pressure amplitude of the harmonic signals was measured. It did not exceed 9% of the amplitude of the fundamental frequency.

Before and after the sonication the temperature of the buffer solutions was measured. Heating from ultrasonic absorption was less than 0.5 K, i.e., negligible.

Results

Membrane conductivity was always in the range of $(6.6 \pm 2)\ 10^{-8}\ \Omega^{-1}\,cm^{-2}$. It was not altered by ultrasound irradiation.

No shift of the potential difference could be measured if the pH electrode was exposed to ultrasound in

the bulk volume. This indicates that sound–electrode interactions do not disturb the experimental results.

The diffusion of acetic acid along a concentration gradient through a BLM causes a pH shift in the USL. Fig. 2 demonstrates examples of pH profiles recorded in the USL of a BLM at pH 8. The ultrasonic field affected the difference ΔpH between the pH values of the bulk and the layer immediately at membrane surface. On the side facing the transducer, in the following called *cis* side, ΔpH was decreased, whereas it was increased at the opposite, i.e. *trans* side. The difference ΔpH across the membrane remained unaffected by the soundwaves.

The thickness of the USL at the *cis* and *trans* sides was diminished by ultrasound. But the sound effect at the *cis* side was much greater than at the *trans* side. These results were independent of the compartment to which the acetate has been added to. The profiles obtained at pH 5 for lower acetate concentrations (1 mM) were similar to those demonstrated in Fig. 2.

All measurements were made in steady state which was achieved shortly after the addition of acetate as a consequence of the agitation by the magnetic stirrer bars. The steady state proton concentration was shifted by ultrasound. After the beginning of each irradiation period the system needed some seconds to reach a new steady state. This shift was entirely reversible.

Fig. 3 gives an example of the time dependence of the proton concentration in a distance of 90 μm from the membrane when ultrasound of different intensities was turned on and off.

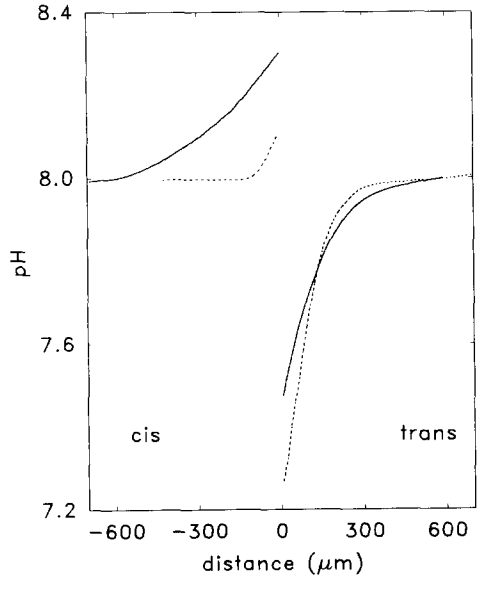

Fig. 2. The concentration of H^+ recorded at both sides of the membrane as a function of the distance to the membrane at pH 8 of the bulk solutions. The solid curves show the profiles under reference conditions the dotted ones in a continuous ultrasonic field of a focussed transducer at 10 MHz and a spatial average pressure of 77 kPa. The concentration of acetic acid at the *cis* side was 60 mM. The ultrasound beam was directed from *cis* to *trans*.

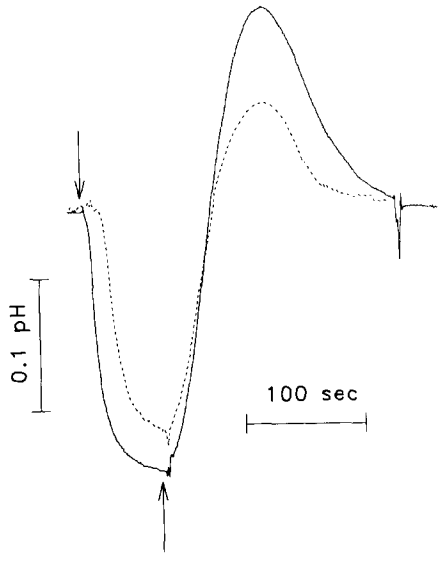

Fig. 3. Change of the proton concentration as function of time. The arrows indicate ultrasound on (first arrow) and off (second arrow), respectively. The microsensor was placed in a distance of 90 μm to the membrane surface in the *cis* chamber where the acetic acid concentration was 20 mM. pH of the bulk 7.5. The direction of sound propagation was from *cis* to *trans*. A plane transducer produced a sound field of 4 MHz and a continuous spatial peak time average pressure of 54 kPa (solid line) and 35 kPa (dotted line).

The steady state H^+ concentration is an exponential function of the distance to the membrane (Fig. 2). Fitting all experimental results as required by Eqn. 2 a good correlation was achieved. The parameters δ and $c_s - c_b$ were used to describe the ultrasound effect. Varying the frequency f in the range from 1 to 12 MHz pH profiles of the *cis* side were recorded at different values of sound pressure. As an example $c_s - c_b$ at the *cis* side was presented as a function of the average sound pressure at 10 MHz (Fig. 4).

The dependence of δ on the reciprocal of the square of the sound pressure p is linear for high pressure values (Fig. 5). The solid line represents δ as expected from the theory (see Discussion).

Detecting δ at the spatial average sound pressure of 50 kPa in analogues figures at all frequencies used, we obtained the dependence of δ on f^{-2} corrected by a theoretical value G (see Discussion) which characterizes the properties of the different transducers (Fig. 6). Again the theoretical values are indicated by a solid line.

The theory developed in the next section does not require any information about the buffer capacity or the absolute concentrations of acetate added. Nevertheless, the concentration profiles shown in Fig. 7 demonstrate that the final thickness of the unstirred layer depends on the concentration gradient also in an

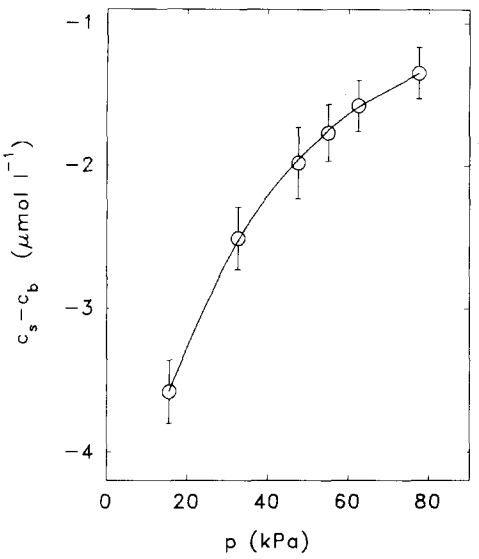

Fig. 4. The difference of the proton concentration values at membrane surface c_s and in the bulk c_b is plotted versus the spatial average time average sound pressure at a sound frequency of 10 MHz (focussed transducer). The *cis* solution contained 1 mM acetic acid. The direction of sound propagation was from *cis* to *trans*. The pH value of the bulk solutions was 5.

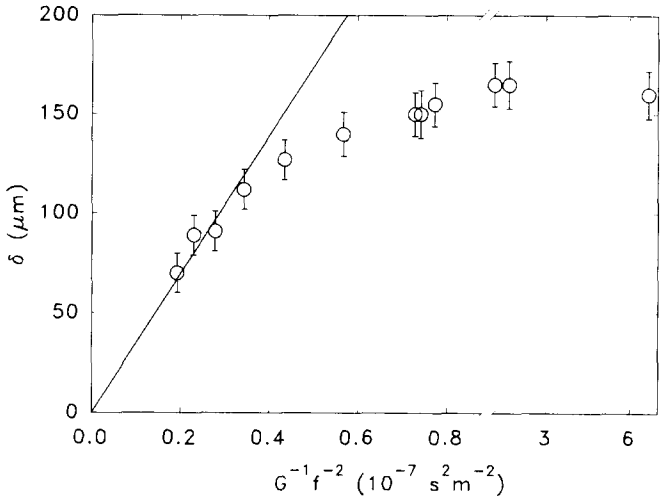

Fig. 6. The dependence of the thickness of the unstirred layer on the frequency f in terms of $G^{-1}f^{-2}$ at a constant spatial average sound pressure of 50 kPa. In order to vary the sound frequency from 1 to 12 MHz in steps of 1 MHz broadband focussed transducers with resonance frequencies at 10 MHz ($G = 3.6 \cdot 10^{-7}$ m^2), 5 MHz ($G = 5.5 \cdot 10^{-7}$ m^2) and 2.25 MHz ($G = 1.5 \cdot 10^{-6}$ m^2) were used. The experimental conditions were the same as in Fig. 4. The slope of the solid line was derived from theory and amounts to $3.48 \cdot 10^3$ m^{3}s^{-2}.

ultrasonic field. The profiles obtained at 1.0 and 70 mM acetate are compared under similar conditions.

Discussion

The value found for membrane conductivity is in accordance with literature data available for phosphatidylcholine/cholesterol model membranes [21,22]. Also, its invariability during sonication was reported earlier [23,9].

The pH difference across the membrane remained constant during sound exposure in comparison to the reference conditions. This agrees with transmembrane potential measurements performed in the presence of a protonophore in an ultrasonic field under similar conditions [9]. In that work it was suggested that the

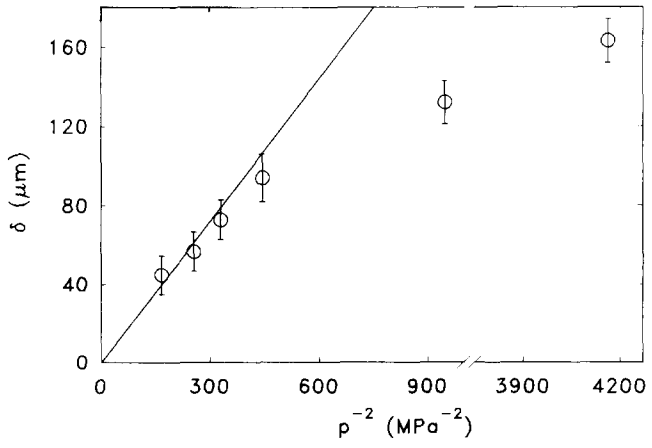

Fig. 5. The size of the unstirred layer δ is plotted in dependence on p^{-2} (spatial average time average sound pressure). The experimental conditions were the same as in Fig. 4. The slope of the solid line was derived from theory and amounts to $2.4 \cdot 10^5$ kg^{2}m^{-1}s^{-4}.

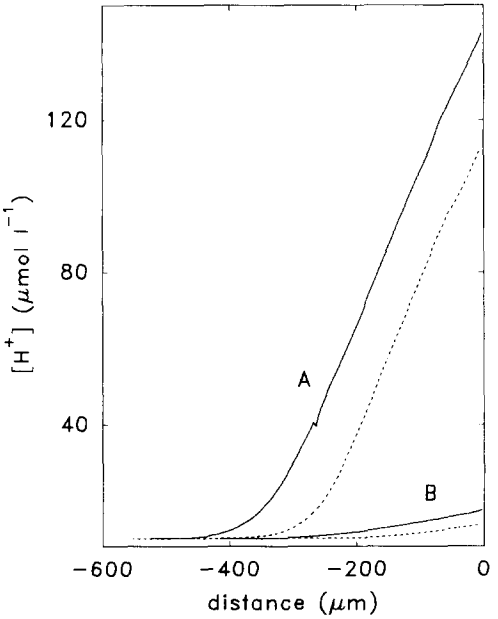

Fig. 7. The concentration of H^+ recorded at the *cis* side of the membrane as function of the distance from the membrane at pH 5 of the bulk volume. The solid line indicates the pH profiles under reference conditions, the broken line shows the profiles during the application of ultrasound. An unfocussed sound transducer transmitting soundwaves from *cis* to *trans* with a peak pressure of 54 kPa at a frequency of 4 MHz was used. The buffer at the *trans* side of the membrane contained acetic acid in the final concentration of: A, 70 mM; and B, 1 mM.

mechanism responsible for the decrease of the USL thickness in an ultrasonic field was an unidirectional fluid flow, the so-called quartz wind, established in front of the transducer. Since cavitation in the exposure chamber near the BLM is not very likely because of the lack of subharmonic signals apart from quartz wind one mechanism for the reduction of the USL is conceivable only: microstreaming due to vibrations of the membrane interacting with the sound wave [24]. However, in the latter case there should be no essential difference between the ultrasound effect on the USL thickness at the *cis* and *trans* side. As seen from Fig. 2 the USL on the *cis* side was much smaller than that on the opposite side. If there was any microstreaming it had no significant influence on our experimental results. Therefore, we suppose that quartz wind is the mechanism responsible for the reduction of the USL in the sound field.

The sound energy absorbed by the buffer solution will partly be transformed into the mechanical energy of the streaming. In water the velocity of the streaming along the sound axes can be calculated according to Liebermann [13]:

$$v = (2+b)\frac{(2\pi f)^2 IG}{\rho u^4} \tag{4}$$

where f, I and u are sound frequency, intensity and velocity, respectively and ρ is the density of water. Factor b is a constant depending on the viscosity of the medium and amounts to 2.4 for water [13]. The geometrical factor G is a function of the size of the sound beam with the radius r_s and the radius of the cylindrical PTFE chamber r_0 [13]:

$$G = \frac{r_s^2}{2}\left(\frac{r_s^2}{r_0^2} - 2\ln\frac{r_s}{r_0} - 1\right) \tag{5}$$

The intensity I determined by a radiation pressure method was substituted by the quotient of the square of the rms pressure p measured with the help of a hydrophone and the characteristic acoustic impedance, i.e., the product of c and ρ [25]. For the transformation we get:

$$v = (2+b)\frac{(2\pi fp)^2 G}{\rho^2 u^5} \tag{6}$$

In Liebermann's equation r_s is the radius of a soundfield with rectangular pressure distribution. In a real sound field generally r_s is assumed to be that radius of the profile where p has dropped to 50% of its peak value on the beam axis.

Although Eqn. 6 was developed for plane transducers it is assumed that it describes also our focused soundfields with sufficient accuracy since the focus length corresponds well with the total length of the PTFE chamber. The precondition that the product of the free propagation length and sound absorption coefficient must be much less than unity is met too. The estimation of v was made regardless of the harmonic content of the sound waves. Due to the neglect an error occurred which was less than 5%.

An additional argument in favor of the quartz wind hypothesis is the way how δ depends on the streaming velocity v. According to the non-slip condition v will decrease within the viscous boundary layer to a value of $v_v(0) = 0$ at the membrane surface. The distance δ_v is defined as the distance from the membrane where v_v equals 99% of v. Schlichting [26] has derived an expression for $v_v(\delta_v)$:

$$v_v(\delta_v) = 1.755\sqrt{a\nu} \tag{7}$$

where ν is the kinematic viscosity of the fluid and a is a constant. a can be determined calculating v_v at a distance δ to the membrane. As far as $\delta \ll \delta_v$ [14] the velocity of the viscous flow near the membrane has to be found as [26]:

$$v_v(\delta) = \frac{h}{2}\frac{a^{3/2}}{\nu^{1/2}}\delta^2 \tag{8}$$

where h is a numerical constant, approximately equal to 1.233 [26]. The unknown velocity $v_v(\delta)$ can be obtained solving Eqn. 3 by means of Eqn. 2 at $x = \delta$:

$$v_v(\delta) = \frac{D}{\delta} \tag{9}$$

Eqn. 3 is valid in the steady state. Fig. 3 shows that ultrasound alters the steady state concentrations. A short period of time after turning ultrasound on the concentration values remained constant.

From Eqns. 6–9 the dependence of δ on the sound parameters can be derived:

$$\delta = \frac{D^{1/3}\nu^{2/3}\rho^2 u^5}{2.14G(2\pi fp)^2} \tag{10}$$

The theoretical and the experimental results are in good agreement at high sound frequencies and high pressure values (Figs. 4 and 5). In order to find the numerical solution of Eqn. 10 for D the value $5 \cdot 10^{-5}$ $cm^2\,s^{-1}$ and for p the spatial average data were inserted.

Figs. 5 and 6 show that δ is not a linear function of p^{-2} and f^{-2} when v is small. This result is not unexpected because it is obvious that the USL should have a finite thickness even if there is no stirring motion at all [17,27].

It can not be excluded that ultrasound decreases the USL adjacent to the pH electrode. However, the effect has been neglected in the considerations made until now because an estimation shows that the size of this

USL should not exceed 10 μm without stirring [10]. Buffer movements due to the magnetic bars reduced this value so that it was small in comparison with the total error of the determination of δ.

Figs. 2 and 7 indicate that the thickness of the USL and ΔpH in the USL strongly depend on the concentration gradient of acetic acid as well as on the buffer capacity, although the stirring conditions have always been kept constant. High concentrations of acetic acid were accompanied by large pH changes in the USL and high values of δ (Fig. 7). These results were found in spite of the fact that the regression coefficient of the curve fitting using Eqn. 2 is not as good as at small concentrations.

Acetate played not only the part of a carrier of protons but increased the buffer capacity too. High buffer capacities decreased the absolute value of the concentration difference $c_s - c_b$ and seemed to enlarge the thickness of the USL (Fig. 2). These observations agree with results obtained by measurements of pH profiles near a membrane [28] and with the decrease of the transmembrane pH with increasing buffer capacity [29].

Summarizing, we conclude that ultrasound induced streaming is able to affect both the thickness of the unstirred layer δ as well as the pH shift ΔpH within the USL. Their final magnitudes are not only a function of the ultrasound field parameters but of their own initial values too.

Acknowledgments

This work has been supported by the German Ministry of Science and Technology (BMFT) 01ZZ9105. One of the authors is indebted to the German Academic Exchange Service (DAAD) for subsidizing his stay at the University Halle.

References

1 Barry, P.H. and Diamond, J.M. (1984) Physiol. Rev. 64, 763–872.
2 Sinisterra, J.V. (1992) Ultrasonics 30, 180–185.
3 Schmidt, P., Rosenfeld, E., Millner, R. and Schellenberger, A. (1987) Ultrasonics 25, 295–299.
4 Schmidt, P., Rosenfeld E., Millner R., Czerner R. and Schellenberger, A. (1987) Biotechnol. Bioeng. 30, 928–935.
5 Dinno, M.A., Dyson, M., Young, S.R., Mortimer, A.J., Hart, J. and Crum, L.A. (1989) Phys. Med. Biol. 34, 1543–1552.
6 Mortimer, A.J. and Dyson, M. (1988) Ultrasound Med. Biol. 14, 499–506.
7 Tyle, P. and Agrawala, P. (1989) Pharmaceut. Res. 6, 355–361.
8 Barannik, E.A., Tovstjak, S.A. and Girnyk V.V. (1987) Biofizika 33, 364–366.
9 Pohl, P., Rosenfeld, E. and Millner R. (1993) Biochim. Biophys. Acta 1145, 279–283.
10 Kaschke, V. and Kuhlmann G. (1980) Enzyme Microb. Technol. 2, 309–312.
11 Antonenko, Y.N. and Bulychev, A.A. (1991) Biochim. Biophys. Acta 1070, 474–480.
12 Dainty J. and House C.R. (1966) J. Physiol. 182, 66–78.
13 Liebermann, L.N. (1949) Phys. Rev. 75, 1415–1422.
14 Pedley, T.J. (1983) Q. Rev. Biophys. 16, 115–150.
15 Mueller, P., Rudin, D.O., Tien H.T. and Wescott W.C. (1963) J. Phys. Chem. 67, 534–535.
16 Gutknecht, J. and Tosteson, D.C. (1973) Science 182, 1258–1261.
17 Antonenko, Y.N. and Bulychev, A.A. (1991) Biochim. Biophys. Acta 1070, 279–282.
18 Preston, R.C. (1991) Output measurements for medical ultrasound, pp. 57–128, Springer, London.
19 Starritt, H.C., Duck, F.A. and Humphrey V.F. (1989) Ultrasound Med. Biol. 15, 363–373
20 Wu, J. and Du, G. (1993) Ultrasound Med. Biol. 19, 167–176.
21 Gutknecht, J. and Walter A. (1981) Biochim. Biophys. Acta, 641, 183–188.
22 LeBlanc, O.H. (1971) J. Membr. Biol. 4, 227–251.
23 Rohr, K.R. and Rooney, J.A. (1978) Biophys. J. 23, 33–40.
24 Nyborg, W.L.M. (1965) in Physical Acoustics. Principles and Methods (Mason W.P., ed.), Vol. II-Part B, pp. 265–331, Academic Press, New York.
25 Lynnworth, L.C. (1989) Ultrasonic measurements for process control, p. 224, Academic Press, Boston.
26 Schlichting, H. (1979) Boundary layer theory, pp. 95–99, McGraw-Hill, New York.
27 Lerche, D.J. (1976) J. Membr. Biol. 27, 193–205.
28 Antonenko, Y.N., Denisov G.A. and Pohl, P. (1993) Biophys. J. 64, 1701–1710.
29 Antonenko, Y.N. and Yaguzhinsky, L.S. (1984) Bioelectr. Bioenerg. 13, 85–91.